Published in final edited form as:
Clin Cancer Res. 2008 November 15; 14(22): 7511. doi:10.1158/1078-0432.CCR-08-0839.

Bortezomib-Mediated Inhibition of Steroid Receptor Coactivator-3 Degradation Leads to Activated Akt

Gustavo Ayala[1,2], **Jun Yan**[3], **Rile Li**[1], **Yi Ding**[1], **Timothy C. Thompson**[2,3], **Martha P. Mims**[4], **Teresa G. Hayes**[4], **Vivian MacDonnell**[2], **R. Garret Lynch**[4], **Anna Frolov**[2], **Brian J. Miles**[2], **Thomas M. Wheeler**[1,2], **J. Wade Harper**[5], **Ming-Jer Tsai**[3,4], **Michael M. Ittmann**[1], and **Dov Kadmon**[2]

[1] Department of Pathology, Baylor College of Medicine

[2] Department of Urology, Baylor College of Medicine

[3] Department of Molecular and Cell Biology, Baylor College of Medicine

[4] Department of Medicine, Baylor College of Medicine

[5] Department of Pathology, Harvard Medical School, Boston, Massachusetts

Abstract

Purpose—To assess the safety of administering bortezomib to patients undergoing a radical prostatectomy, to assess pathologic changes induced by bortezomib in prostate cancer specimen, and to verify alterations by the drug in proteasome protein targets.

Experimental Design—Bortezomib is a proteasome inhibitor that has shown activity *in vitro* and *in vivo* in prostate cancer. We performed a neoadjuvant clinical trial of bortezomib in men with prostate cancer at high risk of recurrence. The primary endpoints were to evaluate safety and biological activity.

Results—Bortezomib is generally safe in the preoperative setting. Antitumor activity was manifested by tumor cytopathic effect, drops in serum prostate-specific antigen in some patients, and increases in tumor apoptosis. This was associated with cytoplasmic entrapment of nuclear factor-κB. We found an unexpected increase in proliferation in treated tissues and *in vitro*. Bortezomib also increased SRC-3 levels and phosphorylated Akt, both *in vitro* and in treated prostate cancer tissues. Knockdown of SRC-3 blocked the increase in activated Akt *in vitro*. Combined treatment with bortezomib and the Akt inhibitor perifosine was more effective than either agent alone *in vitro*.

Conclusion—These data suggest that combined therapies targeting the proteasome and the Akt pathway may have increased efficacy.

Radical prostatectomy is often successful in treating men with clinically localized disease; however, there is still a significant failure rate, particularly in men with adverse clinicopathologic parameters. New therapies for prostate cancer are necessary, as currently no effective adjuvant therapy is available for patients with high risk of recurrence after treatment of localized disease. The advent of new, targeted therapy drugs opens the door to new intervention options. Bortezomib (PS-341; Velcade) is a first generation, reversible, inhibitor

Requests for reprints: Gustavo Ayala, Department of Pathology, Baylor College of Medicine, One Baylor Plaza, Houston, Texas 77030. Phone: 713-798-3705; Fax: 713-798-2720; gayala@bcm.edu.

Note: Supplementary data for this article are available at Clinical Cancer Research Online (http://clincancerres.aacrjournals.org/).

Disclosure of Potential Conflicts of Interest
M.P. Mims received commercial research support from Keryx.

of the 26S proteasome that binds to and inhibits the 20S catalytic core (1,2). The Ubiquitin-Proteasome Pathway degrades short-lived regulatory proteins such as those required for cell cycle progression and proliferation. The 26S proteasome has two components: a 20S catalytic core, which is bound to two copies of the 19S activator. The first step in this proteolytic process is tagging these proteins with ubiquitin molecules targeting them for degradation. The $p21^{Cip1}$ and $p27^{Kip1}$ cell cycle inhibitors are degraded by the ubiquitin-proteasome pathway as is the P53 tumor suppressor protein (3,4). The ubiquitin-proteasome pathway also has indirect effects on transcription. In particular, nuclear factor-κB (NF-κB) activation requires ubiquitin-proteasome pathway degradation of its inhibitor IκB. After stimulation of cells by cytokines and/or growth factors, IκB is phosphorylated by the IKK complex, leading to degradation of IκB by the 26S proteasome. This allows translocation of the NF-κB complex to the nucleus where it can activate transcription of a number of genes that can promote neoplastic progression in prostate cancer. These include Bcl-2, c-*myc*, interleukin-6, interleukin-8, vascular endothelial growth factor, matrix metalloproteinase 9, urokinase-type plasminogen activator, and urokinase-type plasminogen activator receptor (5–9).

Bortezomib is a proteasome inhibitor that has shown activity against a variety of cancer cell lines including prostate cancer cell lines and prostate cancer xenograft models (10,11). The drug also has activity against other solid tumors (2). A phase I study of bortezomib in androgen-independent, advanced prostate cancer showed decreased prostate-specific antigen (PSA) in 2 of 47 patients with stable PSA in 9 of 47, and 2 of 21 patients with measurable disease had partial responses in retroperitoneal lymph nodes (12). Based on the known biology of prostate cancer and the activity of bortezomib in advanced prostate cancer, we did a neoadjuvant bortezomib clinical trial in men with aggressive clinically localized prostate cancer at high risk of recurrence.

Activation of the Akt pathway can limit the effectiveness of many cancer chemotherapies. Steroid receptor coactivator-3 (SRC-3) interacts with steroid receptors and is also overexpressed in prostate cancer patients. Overexpression of SRC-3 correlates well with the prostate cancer proliferation and cell survival (13). Knocking down of SRC-3 in prostate cancer cells leads to decreased cell proliferation, inhibition of cell cycle progression, and increased apoptosis. Most importantly, down-regulation of SRC-3 protein in prostate cancer cell lines results in decreased tumor growth in nude mice. Increased expression of SRC-3 results in up-regulation of the Akt pathway via activation of multiple genes in the Akt pathway. In this study, we have found that although bortezomib does have antitumor activity in prostate cancer, this activity is limited by bortezomib induction of SRC-3 and activation of Akt.

Materials and Methods

Study objectives

The primary objectives are to assess the safety of administering bortezomib to patients undergoing a radical prostatectomy, to assess pathologic changes induced by the drug in prostate cancer specimens, and to verify alterations in proteasome protein targets. This report emphasizes the results of these latter objectives. The secondary is long-term clinical follow-up to assess outcome in comparison with historical controls. We report here our initial observations on the histologic changes and alterations of protein targets in the pathologic specimens analyzed thus far and corresponding *in vitro* work that lends support to these observations. After completion of enrollment, we plan a complete analysis of these variables in all specimens and correlation with clinical response and, ultimately, clinical outcome.

Treatment plan

The study was designed for a total of 40 patients with locally advanced/high-grade prostate cancer. We currently have enrolled 40 patients; 37 patients completed both the protocol and the surgery, and 2 patients are currently undergoing treatment. The biological studies were done on 21 patients. Inclusion criteria were clinical stage T_{1c} or T_{2a} with high-grade disease (Gleason 8–10), or clinical stage T_{2b}–T_{2c} with Gleason grade of 7 and PSA of >10 ng/mL or clinical stage T_3. Patients received bortezomib by i.v. push at a dosage of 1.6 mg/m^2 once weekly for 4 wk followed by radical prostatectomy within 72 h of the last dose. The study was approved by the Baylor Institutional Review Board (IRB H-11047).

Radical prostatectomy specimen processing and morphologic analysis

Whole-mount prostatectomy specimens were reviewed. We identified morphologic changes that were present in prostates treated with bortezomib that were not commonly found in untreated prostate cancers and that were not found in the pretherapy prostate biopsies of the same patients. The tumors were mapped on each whole-mount slide. The changes were mapped on superimposed whole-mount slides by the investigators (Fig. 1).

A tissue microarray (TMA) was built containing benign and cancer tissues from treated patients. Immunohistochemical stains of biomarkers were done on them and compared with a large TMA of radical prostatectomies described previously (13,14). The biological studies were done on 21 patients. Only patients with a Gleason score of 7 or above were used from the control database. Whenever possible and necessary, they were also compared with the preoperative biopsies of the bortezomib-treated patients.

Immunohistochemistry

Immunohistochemistry was done with antibodies against P-Akt (S473), NF-κB, and Ki67 using a standard avidin-streptavidin peroxidase method as described previously (13). The detection of DNA fragmentation was determined *in situ* by the terminal deoxynucleotidyl transferase–mediated dUTP biotin nick-end labeling technique (13).

Assessment of immunostaining

All TMA-stained slides were digitized and quantified using a method previously described (13,14). Each image was interpreted for immunoreactivity using a 0 to 3+ semiquantitation scoring system for both the intensity of stain and percentage of positive cells (labeling frequency %). For the intensity, the grading scale ranged from no detectable signal (0) to strong signal seen at low power (3). A moderate signal seen at low to intermediate power was designated 2, whereas 1 indicated a weak signal seen only at intermediate to high power. Labeling frequency was scored as 0 (0%), 1 (1–33%), 2 (34–66%), or 3 (67–100%). The multiplicative index of intensity and labeling was considered for analysis and was obtained by totaling the scores of intensity and percentage. Apoptotic and proliferative indices were assessed as previously described (13,14).

Cell culture and reagents

Human prostate cancer cell lines DU145, PC3, and LNCaP were maintained in D-MEM/F-12 supplemented with 10% fetal bovine serum and penicillin (100 μg/mL), and streptomycin (100 μg/mL). Bortezomib and perifosine were dissolved in PBS and MG132 was dissolved in DMSO. PC3 prostate cancer cells were treated with 10 nmol/L bortezomib and/or 10 μmol/L perifosine. DU145 prostate cancer cells were treated with 1 μmol/L bortezomib and/or 10 μmol/L perifosine.

Proliferation, apoptosis, and growth assays

DU145, PC3, and LNCaP cells were seeded in 4-well chamber slide the day before treatment at a density of 3×10^4 cells per well. Bortezomib was added to cells for 48 h. Cell proliferation was assessed by the BrdUrd incorporation assay. DU145 cells were seeded in 1-well chamber slide the day before bortezomib treatment. After addition of bortezomib for 48 h, cells were collected and suspended in 0.5 mL of PBS containing 0.1% (v/v) Triton-X100 for preparation of nuclei. The suspension was adjusted to a final concentration of 0.1% (w/v) RNase and 50 μg/mL propidium iodide. The DNA content was measured by flow cytometry, and apoptosis was assessed by the percentage of sub-G_0 cells. Experiments were done in triplicate. DU145 and PC3 cells were seeded at an initial density of 1.5×10^4 per well in the 2-well chamber slide. Twenty-four hours later, bortezomib was added at the final concentration of 0, 0.5, 1, and 2 nmol/L. Viable cell number was determined from the next day (as indicated as day 1) for 6 d by hemacytometer counts of trypan blue–excluding cells. Data are shown as means ± SD ($n = 3$). Each well was counted thrice, and the average cell number was used as this well's cell number. Note that a lower dose of bortezomib is used in these studies than in the biochemical studies because they are carried out on glass slides, and the cells were significantly more sensitive to bortezomib, perhaps due to differences in binding of drug to these two surfaces. To confirm proteasome activity at these concentrations tested for NF-κB cytoplasmic entrapment *in vitro*, DU145 and PC3 cells were seeded in 4-well chamber slide (Lab-Tek I; Fisher Sci.) at the density of 2.5×10^4 per well; 24 h later, 0, 0.5, 1, and 2 nmol/L bortezomib was added to cells. After 48 h of incubation with bortezomib, cells were washed twice with PBS, fixed with 4% paraformaldehyde, at room temperature for 15 min, and permeabilized with 0.2% Triton-X100, at room temperature for 10 min. Cells were rinsed twice with PBS, then incubated with NF-κB (1: 75; p65, sc-8008 from Santa Cruz Bio) for 1 h at room temperature. After rinsing with PBS twice, cells were incubated with FITC-goat anti-mouse IgG (H+L) for 40 min at room temperature. After rinsing with PBS, mounting medium with 4′,6-diamidino-2-phenylindole was added to slides, and NF-κB immunofluorescence was observed under microscope.

Small interference RNA treatment and transient transfection

For the small interference RNA (siRNA) experiments, PC3 and DU145 cells were seeded the night before transfection at such a density that cells reach ~60% to 70% confluence by the time of transfection. siSRC-3 SMART pool (40 nmol/L; Dharmacon) was used for transfection using Lipofectamine 2000 (Invitrogen). SMART pool siRNA control was used as a negative control. Transfected cells were continued in culture for 2 to 3 d before harvesting for further analyses. Subsequently, PC3 and DU145 cells were treated with SRC-3 siRNA for 2 d, then treated with or without bortezomib for another 2 d. The concentration of bortezomib for PC3 cells is 10 nmol/L and 1 μmol/L for DU145. The viable cells were measured by 3-(4,5-dimethylthiazol-2-yl)-2,5-diphe-nyltetrazolium bromide assay.

Western blotting

Immunodetection was done using a primary antibody and peroxidase-conjugated secondary antibody. PC3 cells were lysed in radioimmunoprecipitation assay buffer with protease inhibitors (Roche Diagnostics) at indicated time points. The proteins were resolved by SDS-PAGE and transferred to nitrocellulose. The following antibodies were used for immunodetection: anti–SRC-3 (BD Biosciences), anti-FKHRL1 (Thr32), anti-FKHRL (Upstate), anti-actin, and anti–cyclin D1 (Sigma). Anti-Akt1, anti-pAkt (Ser472), anti-Akt (Thr308), anti-pGSK3/3 (Ser21/9), anti-GSK3, anti-S6 ribosomal protein (Ser240/244), and anti-S6 ribosomal protein antibodies are from Cell Signaling Technology, and anti–C-Myc are from Santa Cruz Biotechnologies. After peroxide-coupled secondary antiserum (Amersham

Pharmacia), bands were detected using an enhanced chemiluminescent detection system (Amersham).

Statistics

All analyses were done with statistical software SPSS 11.0 (SPSS Inc.).

Results

Clinical and pathologic characteristics of patient cohorts

A total of 40 patients have been accrued to date. Patients ranged from 44 to 76 years (mean, 60.2 years); age of patients in the control group ranged from 37 to 80 years (mean, 62 years). To be enrolled, men had to have clinically localized cancers with high risk of recurrence after radical prostatectomy, and the clinical and postoperative pathologic variables are as expected for such men. In the treated group, most tumors were large, and all had established extraprostatic extension.

Side effects

In general, patients tolerated the treatment well, with grade 1 and 2 toxicity. One patient had grade 3 gastrointestinal toxicity and recovered before surgery, another patient developed atrial fibrillation soon after surgery; both cases were possibly related to the study medication. We did not observe any increased surgical morbidity attributable to the study drug.

PSA changes with therapy

Pretreatment PSA, obtained at least 6 weeks after biopsy (15), was available for 8 patients for comparison to preoperative PSA taken immediately before surgery. Two of 8 patients had a >50% decrease in serum PSA after bortezomib treatment, and 3 others had PSA declines of 14%, 25%, and 45%, respectively. Two patients had increases (7% and 14%), whereas 1 had no change. See Supplementary Fig. S1.

Cytopathic effect of bortezomib therapy

Comparison of pretherapy biopsies with their respective posttherapy prostatectomies showed cytopathic changes attributable to bortezomib therapy. Figure 1A shows unaffected prostate cancer. The most characteristic changes identified were cytolysis and nuclear pyknosis (Fig. 1B). The nuclei shrank became pyknotic and acquired a spindled morphology (coma like), in contrast to the normal round/ovoid shape with large nucleoli (Fig. 1B). The cytoplasm of the affected cells has a frothy, foamy, microgranular appearance, with dissolution of the cell membranes. Cytopathic effects were confined to tumor cells, and no visible cytopathic change was noted in benign tissue. The percentage of tumor with visible cytopathic effects was variable. Some tumors had little or no morphologic effect, whereas in other cancer, 10% to 15% of the tumor showed cytopathic effects. Cytopathic changes were found predominantly in the growing edge of the tumor, as seen in Fig. 1C. Pretreatment controls showed no such changes.

Cytoplasmic entrapment of NF-κB after bortezomib therapy

We next analyzed the histologically normal tissues for alterations in the downstream proteasome target NF-κB. Bortezomib effects on the nuclear and cytoplasmic expression of NF-κB were as expected. The mean expression of nuclear NF-κB in prostate cancer was lower in patients treated with bortezomib than comparable patients without treatment from the master TMA database (median, 4 versus 1.5; $P = 0.0020$; Fig. 2A). In contrast, NF-κB cytoplasmic expression was higher in patients treated with bortezomib than controls (median, 0 versus 6; $P < 0.0001$; Fig. 2B).

Effects on growth, apoptosis, and proliferation

Our results on the effect on induction of apoptosis in prostate cancer *in vivo* are in concordance with previously published *in vitro* and preclinical data (16,17). As seen in Fig. 2C, the apoptotic rate in tumors was significantly higher in patients treated with bortezomib compared with similar TMA controls (median, 1.9750 versus 0; $P = 0.0006$). We were also expecting a decrease or no effect on proliferation. Surprisingly, we identified a significantly higher proliferative rate in treated patients (median, 0.32 versus 2.5; $P = 0.0033$). To corroborate these surprising results, we obtained the preoperative biopsies in these same patients (available for 21 patients). The median proliferative index (Ki67 expression) in preoperative biopsies was 0.00, in contrast to 3.35 in the same patient's bortezomib-treated tissues ($P = 0.0097$, Wilcoxon signed-ranks test). The proliferative index in tumors of patients treated with bortezomib increased compared with their matched preoperative biopsies. Note that all patients, except two, have increase in the proliferation index. One had no change and one decreased (Fig. 2D).

Effects of bortezomib on proliferation and apoptosis *in vitro*

To determine if bortezomib had similar effects on proliferation and apoptosis *in vitro*, we examined the effect of varying doses of bortezomib on proliferation (BrdUrd incorporation) in the LNCaP, DU145, and PC3 prostate cancer cell lines. As shown in Fig. 3A, bortezomib treatment increases BrdUrd incorporation in DU145 cells, and increased effects were seen with increased dose (Fig. 3B). Similar results were seen in PC3 and LNCaP cells (data not shown). At the same time, apoptosis, as assessed by flow cytometry, increased with increasing doses of bortezomib (Fig. 3B). Thus, bortezomib can promote both proliferation and apoptosis. To determine the net effect of these processes, growth curves were obtained using DU145 and PC3 cells and analyzed on day 1 through 6. Cells numbers increased with increasing doses (Fig. 3C and D). The differences were significant on day 6 for both cell lines. Decreased proteasome activity at these doses was confirmed by cytoplasmic entrapment of NF-κB using immunnofluorescence as previously described (Supplementary Fig. S2; ref. 18). Furthermore, we show that both C-Myc and Cyclin-D1 are up-regulated in cells treated with bortezomib (Supplementary Fig. S6). This further substantiates our findings of increased proliferation in bortezomib-treated cells.

Effects on the Akt pathway

To determine if the changes in proliferation were mediated by activation of the PI3-kinase/Akt pathway, we analyzed the phosphorylated Akt (P-Akt) content in treated tissues. As shown in Fig. 4A, there was a significant increase in P-Akt expression in PCa treated with bortezomib compared with the controls (median, 3 versus 6: $P = 0.0001$). Subsequently, we analyzed the preoperative biopsies for P-Akt expression. Four patients had similar levels, all of which had initial indices of 9 and could not be higher. All patients that had lower initial indices showed increases in their cytoplasmic expression of P-Akt (Fig. 4B) that were significant on matched pair analysis ($P = 0.0455$).

Bortezomib activates the Akt pathway via increased SRC-3

It is known that SRC-3 is degraded by the 20S proteasome (19) and that SRC-3 can induce the activation of Akt signaling in prostate cancer cell lines (13,20). We therefore evaluated the effect of bortezomib and a second proteasome inhibitor, MG132, on SRC-3 levels in PC3 cells. SRC-3 was significantly induced after 8 hours of treatment with 1 μmol/L bortezomib, and even 10 nmol/L bortezomib was able to significantly induce SRC-3 (Fig. 5A). Similar effects were seen in DU145 cells (data not shown). To examine the activation of the Akt pathway by bortezomib, we carried out a more detailed study in PC3 cells. As shown in Fig. 5B, SRC-3 protein levels are increased by 2 hours of bortezomib treatment, and this is accompanied by increases in Ser473 and Thr308 P-Akt. This is expected because we have shown previously

that SRC-3 can activate the Akt pathway (21). These changes in the Akt pathway were accompanied by increased phosphorylation of Akt targets such as GSK3α (Ser21), GSK3β (Ser9), S6 kinase (Ser240/244; Fig. 5C), and FKHRL (Thr32). Bortezomib is known to increase heat shock proteins such as Hsp90 (22), which can play an important role in cell signaling by promoting conformational integrity of key signaling molecules. Thus, bortezomib might be acting via Hsp90 to increase P-Akt. As shown in Fig. 5B, Hsp90 is increased by bortezomib after 8 hours of treatment. However, P-Akt (Ser473 and Thr308) is increased within 2 hours of treatment, as is SRC-3, arguing that induction of SRC-3 is the dominant mechanism for activation of SRC-3, although Hsp90 activation may play a lesser role in this process. To confirm that SRC-3 was responsible for the increase in P-Akt, we knocked down SRC-3 using siRNA in PC3 cells before treatment with bortezomib (Fig. 5D). Pretreatment with SRC-3 siRNA abolished the ability of bortezomib to increase P-Akt. More importantly, the depletion of SRC-3 in prostate cancer cells augments bortezomib-induced cell death (Supplementary Fig. S4).

To confirm that SRC-3 protein is increased in prostate cancer tissue in men treated with bortezomib, we compared SRC-3 protein levels in treated patients to untreated controls by immunohistochemistry. Both cytoplasmic and nuclear SRC-3 were significantly increased in patients treated with bortezomib as predicted from the known biology of SRC-3 and our *in vitro* results (Supplementary Fig. S5).

Inhibition of Akt activation increases the effectiveness of bortezomib treatment

Our data are consistent with the idea that increased P-Akt, via increased SRC-3 protein levels, decreases the effectiveness of bortezomib therapy. To test this hypothesis, we used the Akt inhibitor perifosine (23), which has shown activity against prostate cancer (23). As shown in Fig. 6A, treatment with both agents is markedly more effective than either agent alone in both PC3 and DU145 cells. This is associated with a complete inhibition of the bortezomib-induced increase in P-Akt in both cell lines (Fig. 6B). We analyzed the data by two-way ANOVA for the experiments for studying the combination agents of bortezomib and perifosine. The cell numbers were logarithmically transformed for stabilizing the variability. For PC3, the cell numbers after treated with either bortezomib alone or perifosine alone were significantly lower than these of control group ($P < 0.0001$ and $P < 0.0001$, respectively). However, there was no statistically significant evidence suggesting that there is any interaction between bortezomib and perifosine for reducing PC3 cell numbers. For DU145, the cell numbers after treated with either bortezomib alone or perifosine alone were significantly lower than these of control group ($P < 0.0001$ and $P = 0.003$, respectively). There was also a statistically significant, synergistic interaction between bortezomib and perifosine for reducing DU145 cell numbers ($P < 0.0001$; Supplementary Fig. S6).

Discussion

A major goal in cancer therapy is to develop targeted agents that disrupt aberrantly regulated pathways in the malignant cell. Bortezomib targets the proteasome pathway, which is up-regulated in prostate cancer and other malignancies. In this neoadjuvant clinical trial of bortezomib in men with aggressive but clinically localized prostate cancer, we found evidence of antitumor activity, with only moderate side effects. This antitumor activity was manifested by histologic evidence of tumor-specific cytopathic effect, significant drops in serum PSA in some patients, and significant increases in tumor apoptosis in treated tumors. This was associated with the predicted cytoplasmic entrapment of NF-κB and loss of nuclear NF-κB. Given the antiapoptotic functions of NF-κB, it is likely that at least some of the increased apoptosis seen *in vivo* is mediated by loss of NF-κB signaling (24).

In addition to the predicted antitumor effects noted above, we identified a significant increase in proliferation as assessed by Ki67 immunohistochemistry in bortezomib-treated patients compared with the TMA database. This was further substantiated by comparing the proliferation rate in the pretreatment biopsies, which were also lower. Ki67 is a marker for cells in proliferation; hence, the most likely explanation is that proliferation is increased in patients treated with bortezomib. An alternative explanation is that the increase in Ki67 protein could be due to inhibition of its breakdown by the proteasome. However, in myeloma cells, treatment with several different proteasome inhibitors led to decreased Ki67 expression, so it seems unlikely that Ki67 is degraded predominantly via the proteasome, although degradation partially via the proteasome cannot be excluded (25). Our *in vitro* data showing increased cell proliferation, as measured by BrdUrd incorporation, argues that in prostate cancer cells, bortezomib can both increase proliferation and apoptosis and the increased Ki67 actually reflects increased proliferation *in vivo*, which is confirmed by the increase in cell number in cells treated with bortezomib. Unfortunately, the low mitotic index of prostate cancer and concerns regarding treating patients with BrdUrd make alternative methods of measuring proliferation *in vivo* problematic.

Activation of the Akt pathway plays a key role in prostate cancer progression by activating multiple antiapoptotic and proliferation-promoting proteins (26). Thus, activation of Akt by bortezomib will almost certainly tend to inhibit the effectiveness of this therapy. A previous study has already shown that bortezomib induces Akt phosphorylation/activation and the Akt inhibitor Perifosine augments bortezomib-induced cytotoxicity in multiple myeloma cells (27).

We previously showed that the expression of SRC-3 is increased in clinically localized human prostate cancers and that increased expression is associated with PSA recurrence (13,28). Additionally, there is a strong correlation of SRC-3 expression in cancer tissue with proliferation and an inverse correlation with apoptosis (13). There is also a very strong correlation between SRC-3 and P-Akt levels in prostate cancer tumors. Finally, it was previously shown that SRC-3 actually increases the expression of Akt in prostate cancer cells (20). Thus, SRC-3 can increase activated Akt activity by increasing Akt protein levels and, based on its known biological activities, P-Akt can in turn increase proliferation and inhibit apoptosis. SRC-3 is degraded by the 20S proteasome by interaction with the nonubiquitin-mediated REG_{γ} pathway and thus should be increased by bortezomib (19), as we showed here, both *in vitro* and in the tissues of treated patients. Thus, whereas proteasome inhibition can enhance apoptosis, it also activates antiapoptotic and proliferative pathways, which may reduce its overall effectiveness.

There are two implications to these findings for clinical use of proteasome inhibitors. First, it is possible that prostate cancers with no or low basal SRC-3 expression may be more sensitive to bortezomib treatment. If true, it would allow for targeted therapy based on preoperative measurements of SRC-3 levels in tumor cells. Second, concomitant treatment with agents that inhibit activity or activation of Akt are likely to enhance the activity of proteasome inhibitors in cancers that express SRC-3, as indicated by the *in vitro* results reported here.

The ultimate clinical utility of neoadjuvant bortezomib in benefiting these patients cannot be assessed currently. Although we are encouraged by the shown antitumor activity, additional follow-up to monitor PSA recurrence rates compared with historical controls is required. It should be noted that a bortezomib is not associated with increased rates of surgical complications such as bleeding, infection, or poor wound healing, so it is safe in the preoperative setting with manageable side effects similar to those reported in nonpreoperative patients. Further preclinical and clinical studies of bortezomib in a neoadjuvant setting, particularly in combination with Akt inhibitors, seems warranted.

Supplementary Material

Refer to Web version on PubMed Central for supplementary material.

Acknowledgments

Grant support: NIH Specialized Programs of Research Excellence CA58204.

References

1. Papandreou CN, Logothetis CJ. Bortezomib as a potential treatment for prostate cancer. Cancer Res 2004;64:5036–43. [PubMed: 15289299]
2. Ludwig H, Khayat D, Giaccone G, Facon T. Proteasome inhibition and its clinical prospects in the treatment of hematologic and solid malignancies. Cancer 2005;104:1794–807. [PubMed: 16178003]
3. Lenz HJ. Clinical update: proteasome inhibitors in solid tumors. Cancer Treat Rev 2003;29:41–8. [PubMed: 12738242]
4. Yin D, Zhou H, Kumagai T, et al. Proteasome inhibitor PS-341 causes cell growth arrest and apoptosis in human glioblastoma multiforme (GBM). Oncogene 2005;24:344–54. [PubMed: 15531918]
5. Suh J, Rabson AB. NF-κB activation in human prostate cancer: important mediator or epiphenomenon? J Cell Biochem 2004;91:100–17. [PubMed: 14689584]
6. McDonnell TJ, Troncoso P, Brisbay SM, et al. Expression of the protooncogene bcl-2 in the prostate and its association with emergence of androgen-independent prostate cancer. Cancer Res 1992;52:6940–4. [PubMed: 1458483]
7. Ellwood-Yen K, Graeber TG, Wongvipat J, et al. Myc-driven murine prostate cancer shares molecular features with human prostate tumors. Cancer Cell 2003;4:223–38. [PubMed: 14522256]
8. Giri D, Ozen M, Ittmann M. Interleukin-6 is an autocrine growth factor in human prostate cancer. Am J Pathol 2001;159:2159–65. [PubMed: 11733366]
9. Giri D, Ittmann M. Interleukin-8 is a paracrine inducer of fibroblast growth factor 2, a stromal and epithelial growth factor in benign prostatic hyperplasia. Am J Pathol 2001;159:139–47. [PubMed: 11438462]
10. Williams S, Pettaway C, Song R, Papandreou C, Logothetis C, McConkey DJ. Differential effects of the proteasome inhibitor bortezomib on apoptosis and angiogenesis inhuman prostate tumor xenografts. Mol Cancer Ther 2003;2:835–43. [PubMed: 14555702]
11. Ikezoe T, Yang Y, Saito T, Koeffler HP, Taguchi H. Proteasome inhibitor PS-341 down-regulates prostate-specific antigen (PSA) and induces growth arrest and apoptosis of androgen-dependent human prostate cancer LNCaP cells. Cancer Sci 2004;95:271–5. [PubMed: 15016328]
12. Papandreou CN, Daliani DD, Nix D, et al. Phase I trial of the proteasome inhibitor bortezomib in patients with advanced solid tumors with observations in androgen-independent prostate cancer. J Clin Oncol 2004;22:2108–21. [PubMed: 15169797]
13. Zhou HJ, Yan J, Luo W, et al. SRC-3 is required for prostate cancer cell proliferation and survival. Cancer Res 2005;65:7976–83. [PubMed: 16140970]
14. Ayala G, Thompson T, Yang G, et al. High levels of phosphorylated form of Akt-1 in prostate cancer and non-neoplastic prostate tissues are strong predictors of biochemical recurrence. Clin Cancer Res 2004;10:6572–8. [PubMed: 15475446]
15. Oesterling JE, Rice DC, Glenski WJ, Bergstralh EJ. Effect of cystoscopy, prostate biopsy, and transure-thral resection of prostate on serum prostate-specific antigen concentration. Urology 1993;42:276–82. [PubMed: 7691013]
16. Matta H, Chaudhary PM. The proteasome inhibitor bortezomib (PS-341) inhibits growth and induces apoptosis in primary effusion lymphoma cells. Cancer BiolTher 2005;4:77–82.
17. Duechler M, Shehata M, Schwarzmeier JD, Hoelbl A, Hilgarth M, Hubmann R. Induction of apoptosis by proteasome inhibitors in B-CLL cells is associated with downregulation of CD23 and inactivation of Notch2. Leukemia 2005;19:260–7. [PubMed: 15565166]
18. Ayala GE, Dai H, Ittmann M, et al. Growth and survival mechanisms associated with perineural invasion in prostate cancer. Cancer Res 2004;64:6082–90. [PubMed: 15342391]

19. Li X, Lonard DM, Jung SY, et al. The SRC-3/AIB1 coactivator is degraded in a ubiquitin- and ATP-independent manner by the REGγ proteasome. Cell 2006;124:381–92. [PubMed: 16439211]
20. Zhou G, Hashimoto Y, Kwak I, Tsai SY, Tsai MJ. Role of the steroid receptor coactivator SRC-3 in cell growth. Mol Cell Biol 2003;23:7742–55. [PubMed: 14560019]
21. Yan J, Yu CT, Ozen M, Ittmann M, Tsai SY, Tsai MJ. Steroid receptor coactivator-3 and activator protein-1 coordinately regulate the transcription of components of the insulin-like growth factor/AKT signaling pathway. Cancer Res 2006;66:11039–46. [PubMed: 17108143]
22. Mitsiades N, Mitsiades CS, Poulaki V, et al. Molecular sequelae of proteasome inhibition in human multiple myeloma cells. Proc Natl Acad Sci U S A 2002;99:14374–9. [PubMed: 12391322]
23. Kondapaka SB, Singh SS, Dasmahapatra GP, Sausville EA, Roy KK. Perifosine, a novel alkylphospholipid, inhibits protein kinase B activation. Mol Cancer Ther 2003;2:1093–103. [PubMed: 14617782]
24. Fahy BN, Schlieman MG, Mortenson MM, Virudachalam S, Bold RJ. Targeting BCL-2 overexpression in various human malignancies through NF-κB inhibition by the proteasome inhibitor bortezomib. Cancer Chemother Pharmacol 2005;56:46–54. [PubMed: 15791457]
25. Zavrski I, Naujokat C, Niemoller K, et al. Proteasome inhibitors induce growth inhibition and apoptosis in myeloma cell lines and in human bone marrow myeloma cells irrespective of chromosome 13 deletion. J Cancer Res Clin Oncol 2003;129:383–91. [PubMed: 12851815]
26. Li L, Ittmann MM, Ayala G, et al. The emerging role of the PI3-K-Akt pathway in prostate cancer progression. Prostate Cancer Prostatic Dis 2005;8:108–18. [PubMed: 15724144]
27. Hideshima T, Catley L, Yasui H, et al. Perifosine, an oral bioactive novel alkylphospholipid, inhibits Akt and induces *in vitro* and *in vivo* cytotoxicity in human multiple myeloma cells. Blood 2006;107:4053–62. [PubMed: 16418332]
28. Yan J, Tsai SY, Tsai MJ. SRC-3/AIB1: transcriptional coactivator in oncogenesis. Acta Pharmacol Sin 2006;27:387–94. [PubMed: 16539836]

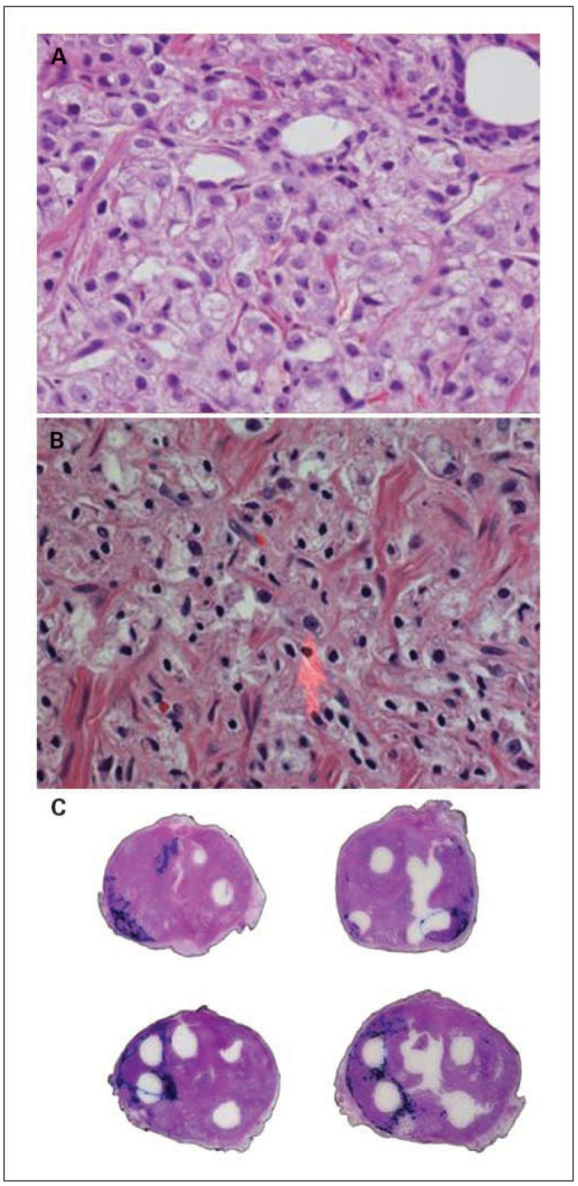

Fig. 1.

Histologic changes associated with bortezomib therapy. *A*, preoperative pretreatment biopsy prostate cancer (untreated controls) is noted in this figure. Note the classic nuclear characteristics of prostate cancer, with large nuclei with open chromatin and large central nucleoli. *B*, histologic changes associated with bortezomib therapy at high power (×400). Note the loss of chromatin detail and nucleoli. The nuclei shrank, became pyknotic, and acquired a spindled morphology in contrast to the normal round/ovoid shape with large nucleoli (*arrow*). The cytoplasm of the affected cells has a frothy, foamy, microgranular appearance, with dissolution of the cell membranes. *C*, whole-mount sections of prostates treated with bortezomib showing areas of tumor cytopathic effect. The tumors are delineated in blue and the areas with therapy related change inside thetumor are dotted in black by the investigator on a superimposed slide. Note that these are mostly located in the peripheral portions of the tumors.

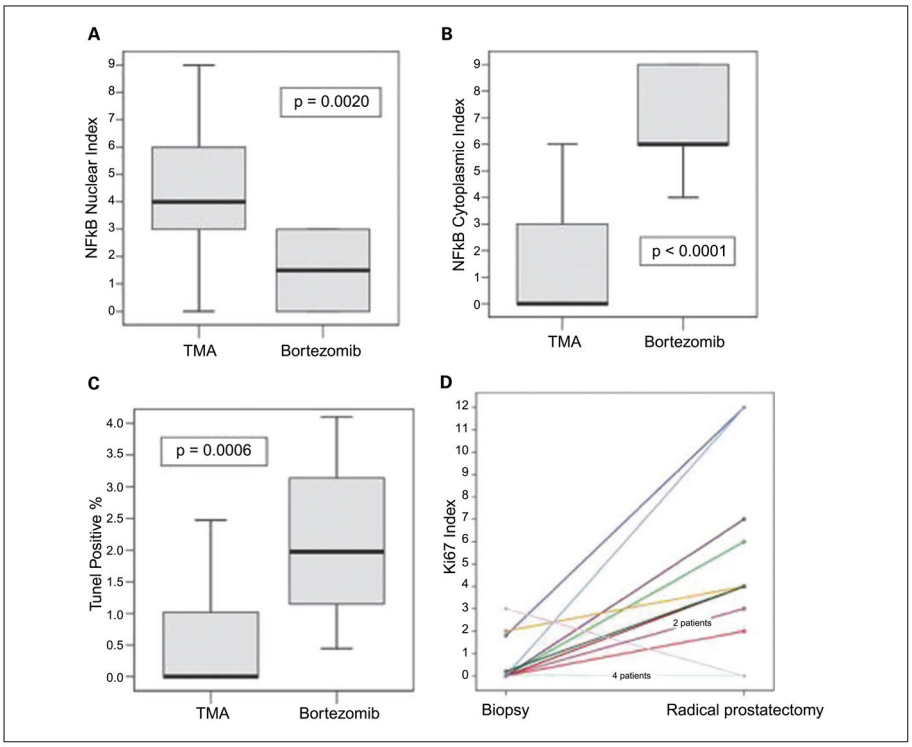

Fig. 2.

Biological effects of bortezomib in prostate cancer tissues. *A* and *B*, cytoplasmic and nuclear NF-κB were quantified using immunohistochemistry as described in Materials and Methods. NF-κB cytoplasmic expression is increased in patients treated with bortezomib (*B*), whereas nuclear expression is decreased compared with controls (*A*). Boxplot shows the median. *C*, apoptotic rate and proliferative index were determined as described in Materials and Methods. Results for patients treated with bortezomib and controls are shown. Boxplot shows the median. *D*, proliferative index in tumors of patients treated with bortezomib (1) compared with their matched preoperative biopsies (0). Note that all patients, except 2, have increase in the proliferation index. One had no change and one decreased.

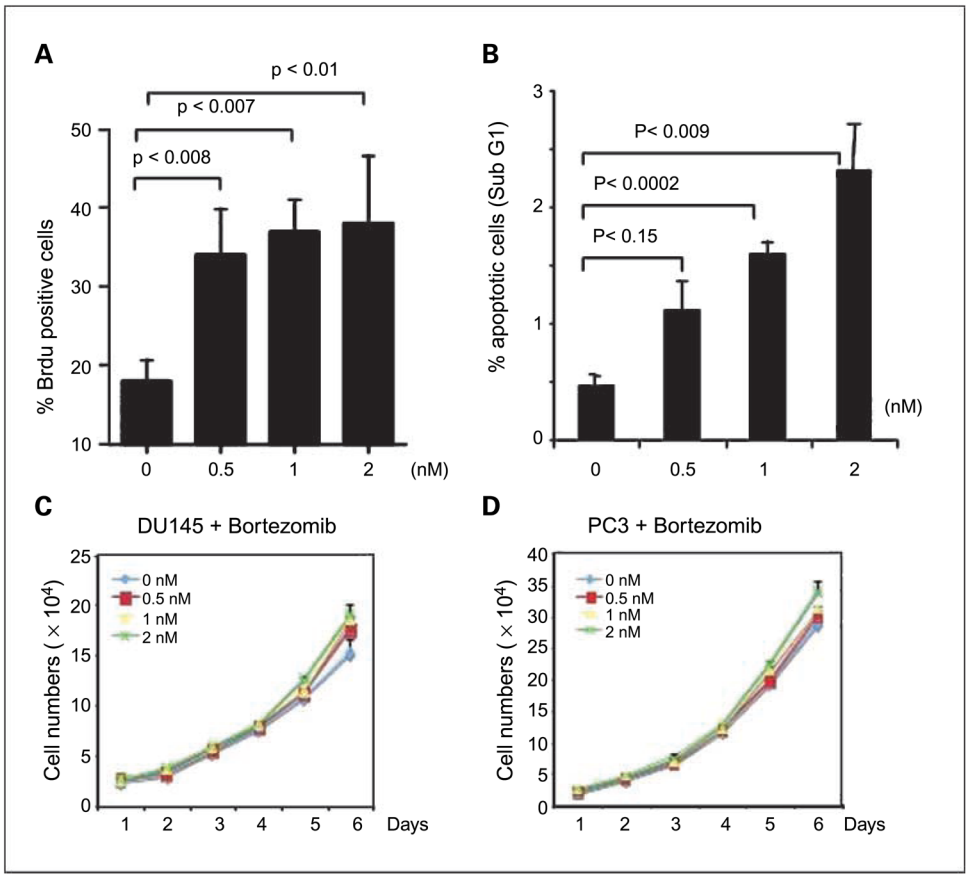

Fig. 3.

In vitro effects of bortezomib on growth, proliferation, and apoptosis. DU145 cells were inoculate in a 4-well chamber slide (Lab-Tek II; Fisher) at a density of 3×10^4 per well and incubated overnight, and bortezomib was added at the indicated concentration for 48 h. BrdUrd labeling and detection was done as described in Materials and Methods. *A*, the percentage of BrdUrd-positive cells represents the average of four random microscopic fields from experiment 2. Columns, mean; bars, SD. 0 μmol/L, 19.5% ± 2.7%; 0.5 μmol/L, 29.6% ± 3.9%; 1 μmol/L, 28.2% ± 5%; 2 μmol/L, 29.8% ± 5.1%. *B*, DU145 cells were inoculated at 1-well chamber slide (Lab-Tek II; Fisher) overnight, and bortezomib was added at the indicated concentration for 48 h. Apoptosis was assessed by the percentage of sub-G_1 cells though DNA content by flow cytometry, relative to untreated cells. Experiments were done in triplicate. Du145 (*C*) and PC-3 (*D*) cells were seeded at an initial density of 1.5 × 104 per well in the 2-well chamber slide. Twenty-four hours later, bortezomib was added at the final concentration of 0, 0.5, 1, and 2 nmol/L. Viable cell number was determined from the next day (as indicated as day 1) for 6 d by hemacytometer counts of trypan blue – excluding cells. Points, mean (n = 3); bars, SD. The differences in growth are more noticeable with increasing time and greater with increasing doses. Differences were significant on day 6.

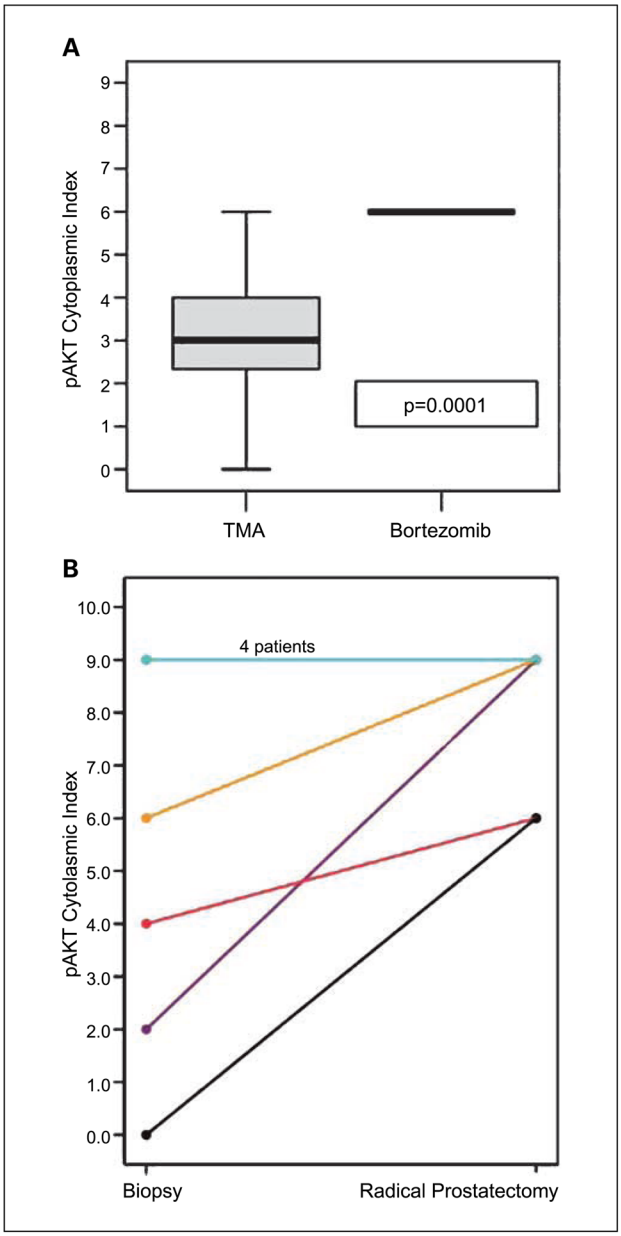

Fig. 4.

Effect of bortezomib on P-Akt *in vivo*. P-Akt was quantified using immunohistochemistry as described in Materials and Methods. P-Akt is increased in the radical prostatectomy tissues of bortezomib-treated patients compared with controls (*A*) and the preoperative biopsies (*B*).

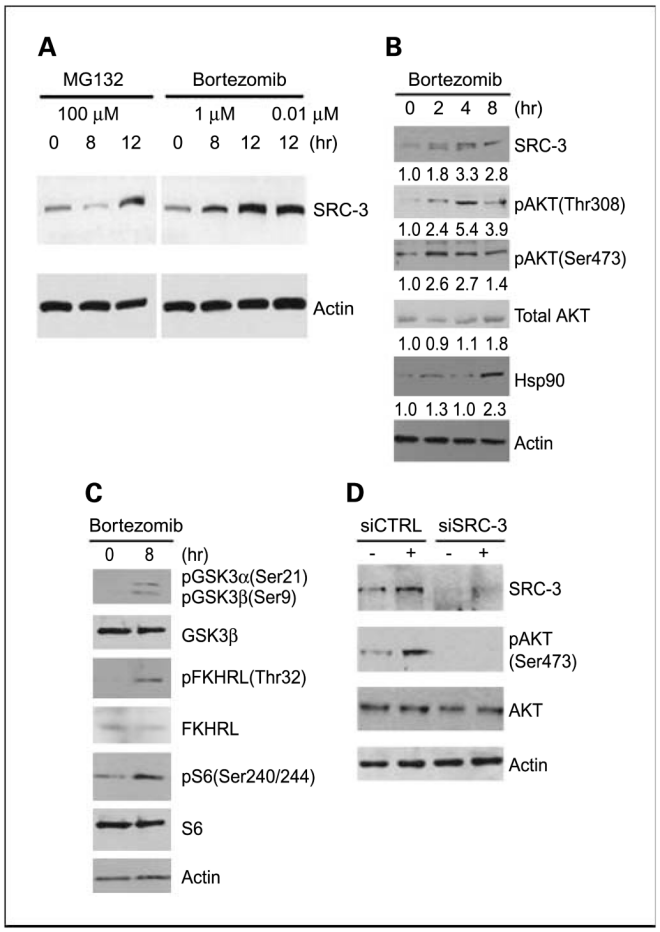

Fig. 5.

Bortezomib increases P-Akt via increased SRC-3. *A*, Western blot showing SRC-3 expression at the indicated time after treatment with MG132 or bortezomib. Actin loading control is shown. *B*, Western blot showing SRC-3, P-Akt (The308 and Ser473), total Akt, and Hsp90 expression at the indicated time after treatment with bortezomib. Actin loading controls are shown. Normalized expression as determined by densitometry relative to time 0 is indicated. *C*, Western blot showing expression of P-Akt target proteins after treatment with bortezomib. Actin loading control is shown. *D*, PC3 cells were pretreated with SRC-3 siRNA or control siRNA for 72 h and then treated with bortezomib for 8 h (+) or vehicle (−). Cell lysates were then prepared and levels of SRC-3, P-Akt (Ser 473), Akt, and actin (loading control) protein determined byWestern blotting.

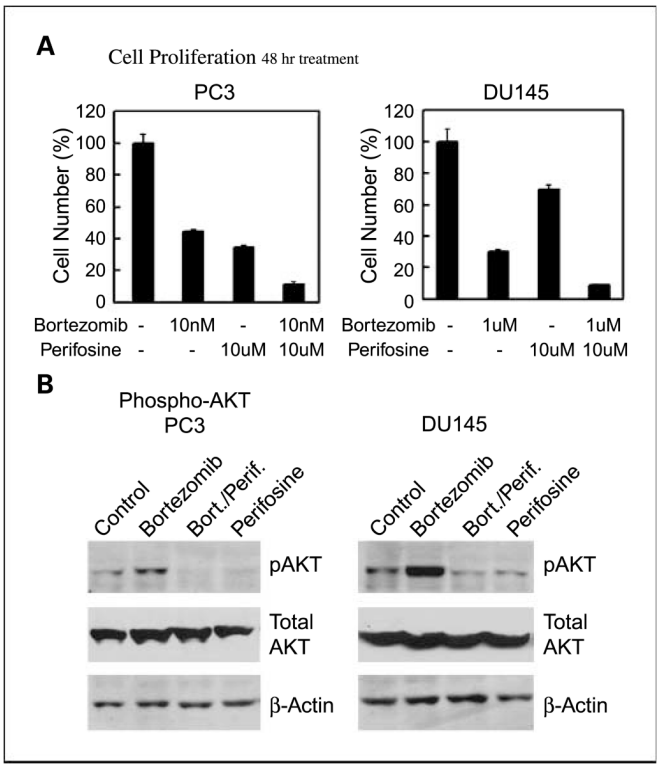

Fig. 6.

Combination treatment of prostate cancer cell lines with bortezomib and perifosine. *A*, PC3 or DU145 cells were treated for 48 h with the indicated concentrations of bortezomib and/or perifosine or vehicle only, and counted after staining with trypan blue. Cell number relative to controls treated with vehicle only (100%) are indicated. *B*, cell lysates were prepared from cells treated as described in (*A*) and levels of P-Akt (Ser 473) determined by Western blotting. Actin loading control is shown. All Figures: Box plots were used for nonparametric data and show the median (line), interquartile range (the box includes the middle 50% of observations), and whiskers extend out to the farthest points that are not outliers. These plots allow the reader to visually compare distributions of the variables.